Relaxation processes and charge transport across liquid crystal-electrode interface

Relaxation processes and charge transport across liquid crystal–electrode interface

A V Koval'chuk

Department of Molecular Photoelectronics, Institute of Physics, National Academy of Sciences, Prospekt Nauki 46, Kiev, 03650, Ukraine

Abstract
At $U < 1$ V nearly the entire voltage in liquid crystals (LC) and in solutions of dyes in LC is applied to the near-electrode regions. In this range of voltages, the Schottky emission through a dielectric layer is the electric current flow mechanism transport. A thin (several nanometres) dielectric layer is formed through adsorption on the electrode of not only ions, but also neutral impurities. According to estimates, the concentration of such molecules in pure LC may much exceed that of ions. It is demonstrated experimentally that the barrier controlling the charge transport lies at the anode and characterizes the ionization of LC molecules. Similarities and distinctions between the observed tunnel charge transport in dielectric liquids and the Schottky effect in solids are analysed. It is shown that the low-frequency dielectric dispersion is caused by voltage redistribution. Comparison of the parameters characterizing the carrier transport with those of the relaxation processes in the diffusion region of the electric double layer shows that long-term near-electrode processes are controlled by charge transport across the electrode–LC interface.

1. Introduction

Dispersion of the complex permittivity components ε' and ε'' in liquid crystals (LC) is observed at low frequencies. Commonly, such a dispersion is related to the influence of electric double layers (EDL) and accounted for by introduction of additional elements into the equivalent circuit of a sample. It had long been assumed that only one additional static (frequency-independent) element is sufficient [1]: the EDL capacitance C_D. Later, it was shown [2, 3] that C_D depends on f in a frequency range wider than that in [1]. Within the framework of the statistical method, the C_D dispersion can be eliminated by increasing the number of equivalent circuit elements, but this leads to ambiguity of the obtained data.

In [2–5], a dynamic technique was proposed for studying the low-frequency relaxation — the low-frequency dielectric spectroscopy (LFDS). In this technique, the low-frequency dispersions ε' and ε'' are regarded as a relaxation process occurring in the near-electrode
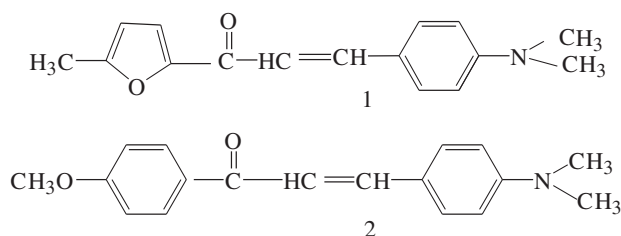
Figure 1. Structural formulas of dyes D_1 (top) and D_2 (bottom).

region. It was also shown that such a process can be analysed in terms of the theory developed for analysis of bulk properties of solids and liquids.

LFDS studies [2–8] have shown that the near-electrode relaxation processes in LC have exceedingly long duration (tens and hundreds of seconds, and even more). Our previous study [8] demonstrated that such relaxation times are much longer than those associated with the transport of individual ions in the near-electrode layer (whose thickness ranges from several to tens of nanometres). At low ion concentration in LC ($10^{20}-10^{21}$ m^{-3}), collective processes of charge redistribution are also unlikely. Therefore, the most probable mechanism of long-term near-electrode relaxation may be associated with charge transport across the electrode–LC interface. Indeed, as shown for the first time in [9], the charge transport across such an interface has tunnel nature and is described as the Schottky emission through the dielectric layer. However, it remained unclear as to how typical of LC is such a charge transport mechanism and how this process is related to near-electrode relaxation processes.

Therefore, the present study was aimed (i) to determine the extent to which the charge transport mechanism proposed in [9] is common to LC and (ii) elucidate the nature of long-term near-electrode relaxation processes by comparison of parameters characterizing these processes with those describing the low-frequency dispersion of ε' and ε''.

To solve these problems, it was necessary to have means to affect the parameters of the electrode–LC interface. Previously, these parameters were considered to be governed by the concentration and type of adsorbed ions. One more goal of this study was to demonstrate that the properties of the near-electrode region depend on the presence of neutral impurities in LC.

2. Materials and experimental procedure

The following LC mixtures were studied: BL055 (B) and ZL1-4803-000 (Z) (both manufactured by Merck Ltd.) At 20 °C, $\varepsilon_\perp = 6.00$, $\Delta\varepsilon = +13.42$ for B, and $\varepsilon_\perp = 11.3$, $\Delta\varepsilon = 51.5$ for Z. Dyes D_1 and D_2 were used as neutral impurities. The structural formulas of these dyes are shown in figure 1. Our study demonstrated that D_1 and D_2 dissolve in B and Z in amounts of up to 5 wt % at $T = 294$ K.

The design of the measuring cell and the method of its filling with the substances to be studied were described elsewhere [2]. Conducting In$_2$O$_3$ layers deposited onto glass substrates were used as electrodes. It was found that for clean In$_2$O$_3$ surfaces the alignment of B and Z molecules is nearly homeotropic. Rubbed polyimide (RP) was used as an orientating agent causing planar orientation of molecules. The sample thickness d was $10-50\,\mu$m. Measurements were mostly done on samples with $d \approx 20\,\mu$m.

The current flow mechanism in the samples studied was determined by analysing current-voltage ($J-V$) characteristics. The $J-V$ characteristics were measured with dc voltage applied to the sample. The experiments showed that the current flowing through a sample

substantially decreases with time (by more than an order of magnitude). Therefore, the dependence of the steady-state current density J_{ST} on voltage U was analysed. In addition, the maximum reverse current density J_{RM} was measured for each voltage U by short-circuiting with the measuring instrument a sample in which a steady-state current J_{ST} flowed.

The parameters of the relaxation processes in the near-electrode regions were determined by LFDS [5, 7–9]. The same technique was employed to measure the ac conductivity σ_{ac}. In the liquid structures under study, an external electric field can essentially affect the parameters. Therefore, data obtained under identical conditions were selected for analysis. It was also found that the presence of a dye results in smaller (2–4-fold) change in the parameters of the structures in question under the action of an external electric field. Therefore, data obtained for solutions of dyes in LC were generally used for analysis.

Measurements were done both at room temperature and at higher temperatures. For temperature studies, the sample parameters were stabilized by keeping the samples under a dc voltage of $\sim$10 V for a long time (several hours) at 50$-$60 °C.

The temperature was maintained constant to within 0.2 K by using a specially designed thermostat with low electromagnetic noise level.

3. Experimental results

As a preliminary in analysing of the mechanism of charge transport across the electrode–LC interface, let us consider the conductance of the LC itself. Thoroughly purified LCs, as also other dielectric liquids, have very low electronic conductivity ($\sigma < 10^{-17}\,\Omega^{-1}\,m^{-1}$) [5], their intrinsic ionic conductivity being much higher ($\sigma \approx 10^{-10}-10^{-12}\,\Omega^{-1}\,m^{-1}$) [10]. In industrially manufactured single-component liquid crystals, σ is generally greater than the intrinsic ionic conductivity owing to the presence of impurities. Since most of electrooptical effects do not necessarily require very low conductivities, no thorough LC purification was carried out, leading to much higher LC cost. For the mixtures under study, prepared on the basis of single-component LC, σ is even greater because of the presence of polar components making higher the $\Delta\varepsilon$. In storage, the impurity ionic conductivity of LCs grows owing to the formation of readily dissociating photooxidation products and complexes arising in diffusion of gases from the atmosphere. Therefore, in most of the LCs studied, σ may substantially exceed (by 3–4 orders of magnitude) the intrinsic ionic conductivity.

In liquid organic electrolytes, the charge exchange at the interface with the electrode is known to occur as a result of redox processes [11]. Cyclic voltammograms of $Z + 2$ wt % D_2 with RP and Cu-electrodes were studied in [9]. No current peak was observed even at very small (0.46 mV s^{-1}) rates of voltage rise and decrease. This fact indicates that redox processed do not play any essential role in structures under study. An analysis of the recorded cyclic voltammograms (dynamic $J-V$ characteristics) showed that at $U < 1$ V the current depends on voltage nonlinearly. To elucidate the current transport mechanism, it was first necessary to determine what is the origin of this nonlinearity — bulk or surface properties of the samples. This was already discussed briefly in [9]. However, to gain a better understanding of the mechanism of charge transport across the electrode–LC interface and the nature of long-term near-electrode relaxation processes, this problem should be discussed in more detail.

3.1. Voltage redistribution

If the $J-V$ nonlinearity is due to near-electrode processes, this must result in a nonuniform distribution of the internal electric field. For structures with ionic conductance, the basic reason for electric field redistribution in a sample is the separation of ions at the electrode.

Such a separation gives rise to an internal electric field directed against the external field. This internal field can be determined in a number of ways. The most precise analysis should take into account both the kinetic processes of ion motion under the action of the electric field and the diffusion of carriers under a concentration gradient [12]. In this approach, to determine the electric field strength even within the roughest approximation, it is necessary to know the concentration, mobility and diffusion constant for ions of different types and signs. Measuring such parameters for LCs is a rather problematic task, since it is still unclear how the concentrations of cations and anions can be determined separately.

Therefore, we used in this study a simpler approach consisting in that the redistribution of voltage, rather than that of the electric field strength is analysed. Hereinafter, the voltage applied to the near-electrode region will be referred to as the 'polarization voltage'. This voltage is equal in magnitude to the internal voltage generated upon charge redistribution at the electrode. The voltages applied to each of the near-electrode layers may be different. Since, by definition, the polarization voltage is the sum of these voltages, the analysis presented below will be also valid for asymmetric properties of the near-electrode layers.

Analysis of the experimental data shows that $J-V$ characteristics are linear at $U > 1$ V. Therefore, it can be taken that, for any voltage, the bulk resistance R of the sample is independent of U. Then the current kinetics can be described by the following expression:

$$J = \frac{U - U_{P\tau}}{RS} \tag{1}$$

where $U_{P\tau}$ is the polarization voltage at a given instant of time and S is the electrode area. At the instant when the voltage is switched off, $U_{P\tau} = 0$. Further, $U_{P\tau}$ increases with time and the current decreases. After $U_{P\tau}$ reaches its peak value U_P, the current stops changing. Therefore,

$$J_{ST} = \frac{U - U_P}{RS} . \tag{2}$$

Immediately after the voltage is switched off (or, in some cases, somewhat later) a maximum reverse current arises with a magnitude

$$J_{RM} = \frac{U_P}{RS} . \tag{3}$$

Relations (2) and (3) yield

$$U_P = U \frac{J_{RM}}{J_{RM} + J_{ST}} . \tag{4}$$

Figure 2 shows the dependence of U_P/U on U for an In_2O_3-Z+2-wt-%-D_2-In_2O_3 sample (homeotropic alignment of molecules). It is clear that, as in the case of RP-Z+2-wt-%-D_2-RP [9], $U_P = 0.998\,U$ at $U < 1$ V, i.e., almost the entire voltage is applied to the near-electrode region. Practically the same U_P/U dependence was obtained for other samples.

The $U > 1$ V range of voltages will not be analysed in detail, especially as an ohmic $J-V$ dependence is observed for these U (see above). Mention should only be made of the fact that at $U > 1$ V the U_P/U ratio depends on the LC type, molecular orientation and dye concentration.

Thus, the presented data demonstrate that at $U < 1$ V the $J-V$ characteristics are governed by the mechanism of charge transport across the electrode–LC interface. The virtually similar dependences of U_P/U on U for all the structures studied suggest that this is due to the same carrier transport mechanism. In order to study the transport of charge carriers across the interface, we must know the bulk electrical properties of the sample.

According to the model considered above, a voltage $U - U_P$ will be applied to the sample. Therefore, we can determine the dc conductivity σ_{dc} from the known J_{ST} value: $\sigma_{dc} =$
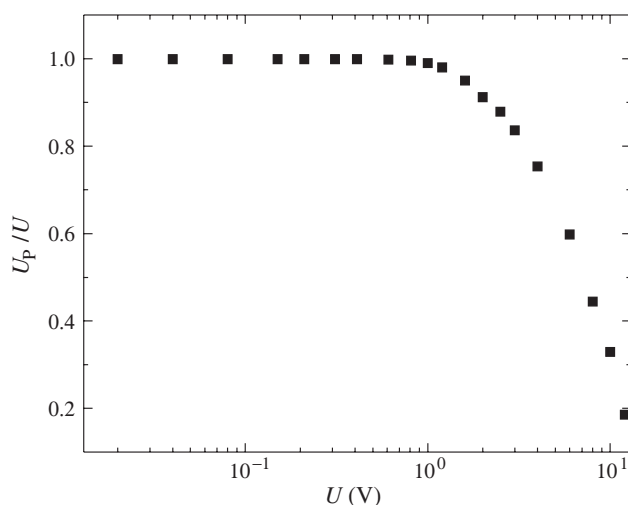
Figure 2. U_P/U versus U for Z+2-wt-%-D_2 with symmetrical SnO_2 electrodes; $d = 19.7\,\mu$m, $T = 292$ K.

$5.7 \times 10^{-7}\,\Omega^{-1}\,\text{m}^{-1}$ for In_2O_3-Z+2-wt-%-D_2-In_2O_3 samples and $\sigma_{dc} = 4.8 \times 10^{-7}\,\Omega^{-1}\,\text{m}^{-1}$ for RP-Z+2-wt-%-D_2-RP. Values of the same order of magnitude were obtained for pure LC and solutions of D_1 and D_2 in B. The presented data indicate that the LCs under study and their solutions with dyes have conductivity exceeding that for well-purified single-component LC by several orders of magnitude. As already mentioned, the possible main reason for the high σ_{dc} is the presence of polar additives making greater the $\Delta\varepsilon$. The σ_{dc} values obtained in this study are of the same order of magnitude as those reported in the literature.

In$_2$O$_3$-Z+2-wt-%-D_2-In_2O_3 and RP-Z+2-wt-%-D_2-RP structures have different molecule alignments. This furnishes an opportunity to estimate the anisotropy of the electrical conductivity of the Z+2-wt-%-D_2 solution. The ratio of the σ_{dc} values is 1.2, which practically coincides with the data for most of other LCs [10].

To confirm the validity of the above analysis of voltage redistribution at the LC–electrode interface, we are to determine σ_{dc} using an alternative method. This can be done in the simplest way when there is no voltage redistribution. Such a condition can be met in the ac case. Therefore, before analysing in detail the mechanism of charge transport across the LC–electrode interface, let us consider the frequency dependences of ε' and ε'' in the samples under study.

3.2. Frequency dependences of ε' and ε''

From section 3.1 follows that the electric field is distributed within the samples nonuniformly. Therefore, it is not quite correct physically to use in analysis of relaxation processes such parameters as ε' and ε'', since they may characterize, depending on frequency, either bulk or surface properties of samples. It would be more correct to employ, e.g., R and C values. However, the analysis would be based in this case on the relations little used in dielectric spectroscopy. It is to enable the application of the relations conventional for the dielectric spectroscopy that the relaxation processes were analysed on the basis of frequency dependences of ε' and ε''.

Figure 3 presents frequency dependences of ε' (1) and ε'' (2) for an RP-Z+2-wt-%-D_2-
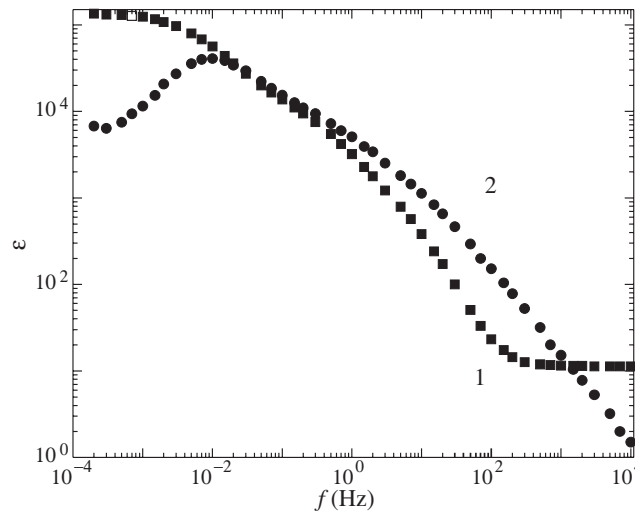
Figure 3. Frequency dependences of ε' (■) and ε'' (●) for an RP-Z+2-wt-%-D$_2$-RP sample ($d = 20.5\,\mu$m) at $T = 292$ K.

RP sample. A rather pronounced low-frequency dispersion is observed at $f < 10^3$ Hz. An essential specific feature of such a dispersion is that the values of ε' and ε'' are very high (about 10^5 for the lowest frequency). This may be due to nonlinear polarization processes and the nonuniform distribution of the field in the sample, mentioned above. Since ε' and ε'' are found at each of the chosen frequencies by analysis of oscillograms, the frequency spectrum of the current flowing through the sample can be monitored. It is known that the frequencies of the harmonics observed in nonlinear polarization must be multiples of the measuring signal frequency. It was shown in [13] that the harmonic with frequency twice that of the measuring signal must have the greatest amplitude in the frequency spectrum. Our study demonstrated that the peak intensity of this harmonic does not exceed the measurement error (less than 1% relative to the signal amplitude at the basic frequency). Hence follows that the main reason for the high ε' and ε'' values is the nonuniform electric field distribution.

As shown above, in the dc case, practically the entire voltage is applied to the near-electrode region at $U < 1$ V. Since the peak value of the measuring signal U_0 is 0.25 V, this gives good reason to maintain that the entire voltage is applied to the near-electrode layer at low frequencies. At those frequencies where there is no low-frequency dispersion ($f > 3 \times 10^2$ Hz), the field in a sample is uniform. With decreasing frequency, the field starts redistributing in such a way that the lower the frequency, the smaller the part of the near-electrode layer to which the voltage is applied. At $f = 0$, the field is applied to a near-electrode layer with thickness equal to that of the dense part of EDL. The capacitance measured at such frequencies will be the capacitance of the near-electrode region, rather than that of the whole sample. Therefore, to determine ε, we should take the thickness of this region W rather than that of the whole sample. However, determining W requires a detailed analysis of the frequency dependences of ε' and ε''. Therefore, ε' and ε'' were determined in a uniform electric field. This was the main reason for the high ε at low frequencies.

Thus, lowering the frequency f in the low-frequency dispersion domain results in that the thickness of the near-electrode region, to which the electric field is applied, decreases. Therefore, an analysis of frequency dependences of ε' and ε'' is practically a scan of the

near-electrode region across its thickness.

The second aspect of the LFDS method [2, 3] is that different near-electrode relaxation processes must differ in their relaxation times (time-frequency scanning). Indeed, as follows from figure 3, two relaxation processes can be observed in the frequency dependences of ε' and ε''. On the basis of the Cole–Cole diagram analysis such a low-frequency dispersion of ε' and ε'' can be described as

$$\varepsilon^* = \varepsilon_{1\infty} + \frac{\varepsilon_{1S} - \varepsilon_{1\infty}}{1 + i\omega\tau_1} + \frac{\varepsilon_S - \varepsilon_\infty}{1 + (i\omega\tau)^{1-\alpha}} \tag{5}$$

where $\omega = 2\pi f$ is the circular frequency; ε_∞ and ε_S are dielectric constants at $f = \infty$ and $f = 0$, respectively; τ is the dielectric relaxation time; and α is the Cole–Cole parameter.

Subscript '1' in expression (5) refers to a higher-frequency relaxation process. Such a process is described by the Debya equation. This low-frequency process was studied in [2] for the first time. Further investigations demonstrated that the low-frequency dielectric relaxation of this type is only observed in LCs with planar or inclined orientation, being due to local changes in molecule orientations (surface dynamic Freedericksz effect [14]). For the data presented in figure 3, $\tau_1 = 0.18$ s. This value is of the same order of magnitude as those obtained for other LCs [2, 14].

In In_2O_3-Z+2-wt-%-D_2-In_2O_3 structures, as also in some other homeotropically aligned LCs or solutions, a dispersion was observed caused by charge transport through the bulk of a sample [7]. This process, as well as the surface dynamic Freedericksz effect, is little related to charge transport across the electrode–LC interface and, therefore, will not be discussed in detail. It is worth noting, however, that low-frequency relaxation processes discussed above are only observed when certain conditions are fulfilled (planar or inclined orientation for the surface Freedericksz effect; relatively weak smearing of the charge packet for the low-frequency relaxation process associated with charge transport).

Let us consider in more detail the basic characteristics and parameters of relaxation processes occurring in the diffusion region of EDL. Such a dispersion is observed in all frequency dependences of ε' and ε'' and is described by the Debya equation, modified by Cole–Cole, with a symmetrical distribution of relaxation times [3, 5]. For the data in figure 3, $\tau = 0.18$ s and $\alpha = 0.14$.

ε_S corresponds to the capacitance of the EDL diffusion region at $f = 0$. Therefore, its value allows us to determine the thickness W of this region. As it was done in [2, 3], we make the following assumptions: in samples with identical electrodes, EDLs with similar parameters are formed near each electrode; the dielectric constant in the EDL is equal to that in the bulk of the sample. Then,

$$W = 2d \frac{\varepsilon_\infty}{\varepsilon_S}. \tag{6}$$

The values of W, τ and α for the samples studied are listed in table 1. It can be seen that the parameters more depend on the orientation of molecules than on the dye concentration. As follows from figure 3, ε' is frequency-independent at $f > 3 \times 10^2$ Hz. In this region, the sample resistance is frequency-independent too. Therefore, it can be taken equal to the bulk resistance and used for calculating the ac conductance σ_{ac}. The obtained σ_{ac} values are listed in table 1. It can be seen that σ_{ac} is practically equal to σ_{dc}. This fact confirms the above-proposed model for determinig the voltage redistribution in the bulk of the sample. The obtained data also indicate that the σ_{ac} ratio is 1.2, similarly to σ_{dc}. Table 1 shows that, upon introduction of 0.8 wt % D_1 dye into B, σ_{ac} even decreases somewhat. Introduction of 2 wt % D_2 into Z results in a less than twofold increase in σ_{ac}. Hence follows that the molecules of dyes D_1 and D_2 are practically neutral in the LC mixtures studied.

Table 1. Parameters characterizing near-electrode relaxation processes at the LC–electrode interface in relation to LC type and presence of neutral dye impurities.

Sample	Electrode	σ_{ac} $(\Omega^{-1}\,m^{-1})$	τ (s)	W (nm)
B	In_2O_3	1.4×10^{-7}	1.5	45
B+0.8 wt % D_1	In_2O_3	1.1×10^{-7}	1.6	44
Z+2 wt % D_2	RP	5.6×10^{-7}	18.2	2.3
Z+2 wt % D_2	In_2O_3	6.7×10^{-7}	3.2	2.7
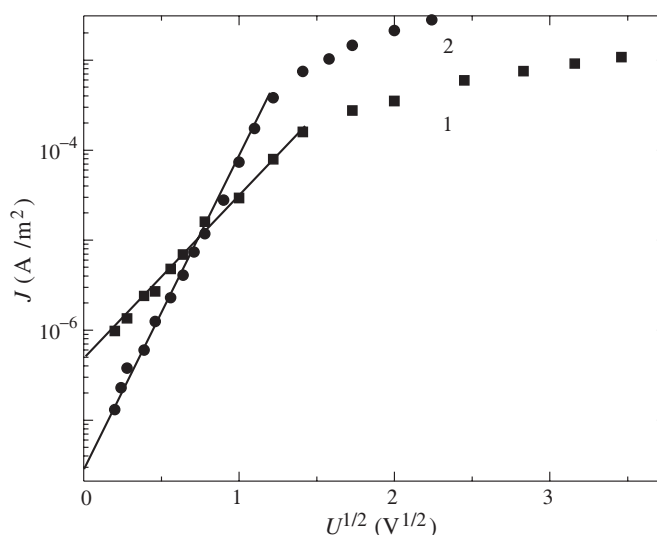
Figure 4. $J-V$ characteristics of B (■) and B+0.8-wt-%-D_1 (●) samples; $d \approx 20\,\mu m$; $T = 292$ K.

A study of the frequency dependences of ε' and ε'' not only confirmed our conclusions made by applying the described the method to determine the voltage redistribution, but also indicated once more that the parameters describing the low-frequency relaxation are closely related to those describing the charge transport across the electrode–LC interface. Therefore, let us consider such a process in more detail.

3.3. $J-V$ characteristics for $U_1/U \approx 1$

Figure 4 presents $J-V$ characteristics of In_2O_3-B-In_2O_3 and In_2O_3-B+0.8-wt-%-D_1-In_2O_3 structures. It is seen that, as in the case of RP-Z+2-wt-%-D_2-RP [9], at $U < 1$ V the experimental data can be approximated by

$$J = J_0 \exp\left(\beta U^{1/2}\right) \tag{7}$$

where β and J_0 are coefficients listed for each sample in table 2. It can be seen that the introduction of dye makes β and J_0 higher. To account for the observed effects, it was important to verify the reproducibility of the results in repeated measurements of $J-V$ characteristics. As is clear from table 2, the values of β and J_0 for solutions of dyes in LCs change to a lesser extent than those for pure LC. The smallest change in β and J_0 in repeated $J-V$ meassurements was observed for RP-Z+2-wt-%-D_2-RP. Therefore, we mainly analyse the charge transport mechanism on the basis of the data obtained for these samples.

Table 2. Parameters characterizing charge transport across the LC–electrode interface in relation to LC type, presence of neutral dye impurities and action of external electric field. Repeated measurements of $J-V$ characteristics were made at the same polarity of applied voltage.

Sample	Electrodes	Run No	d (μm)	β ($V^{-1/2}$)	J_0 ($A\,m^{-2}$)	d_d (nm)
B	In_2O_3	1	19.2	7.3	1.2×10^{-8}	29
B	In_2O_3	2	19.2	4.0	5.1×10^{-7}	95
B+0.8 wt % D_1	In_2O_3	1	18.6	12.2	8.2×10^{-8}	10
B+0.8 wt % D_1	In_2O_3	2	18.6	7.8	2.2×10^{-7}	25
Z+2 wt % D_2	RP	1	20.5	7.8	8.7×10^{-9}	3.2
Z+2 wt % D_2	RP	2	20.5	6.4	2.0×10^{-8}	4.9
Z+2 wt % D_2	In_2O_3	1	19.7	5.8	1.5×10^{-7}	1.1
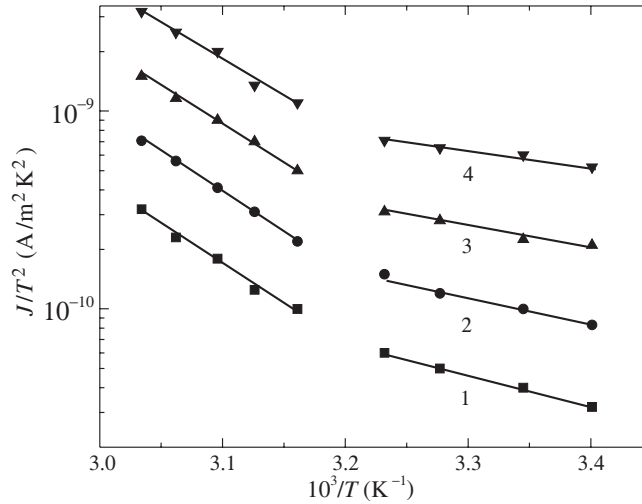
Figure 5. Temperature dependences of J/T^2 for Z+2-wt-%-D_2 structures with symmetric RP-electrodes at U (V): 0.61 ($\blacksquare$), 0.81 ($\bullet$), 1.0 ($\blacktriangle$) and 1.2 ($\blacktriangledown$). $d = 20.5\,\mu$m.

4. Discussion

Expression (7) describes the tunnel current flowing through a dielectric layer [9, 15]. To specify the charge transport mechanism, we studied the temperature dependences of J/T^2 at various U, as it was done in [9]. The data obtained for RP-Z+2-wt-%-D_2-RP structures are shown in figure 5. It is seen that in the temperature range in which the mesomorphic phase exists, $\lg(J/T^2)$ linearly depends on T^{-1}. This gives reason to state that the currents flowing across the electrode–LC interface are governed by the Schottky emission. For this mechanism we have

$$J_0 = A^* T^2 \exp\left(-\frac{e\varphi_B}{kT}\right) \tag{8}$$

where A^* is the Richardson constant, e is the electron charge, φ_B is the barrier height, and k is the Boltzmann constant.

Analysis of the data in figure 5 indicates that the barrier height $\varphi_{BN} = 0.39\pm0.05$ V for the nematic phase (planar orientation of molecules) and $\varphi_{BI} = 0.93\pm0.05$ V for the isotropic phase. Since the charge transport occurs as a result of tunnelling through the dielectric layer, there

are no direct ion–electrode contacts (which is confirmed by cyclic voltammetry). Therefore, a barrier may arise both in charge transport from an electrode to LC (injection) and in back motion from LC to the electrode (ionization). Each of the above processes is characterized by its own barrier height. However, it would be expected that these barrier heights are markedly different.

The temperature dependence of J/T^2 was studied for a Cu-Z+2-wt-%-D$_2$-RP sample in [9] at different voltage signs at electrodes. For '−'Cu-Z+2-wt-%-D$_2$-RP'+', the slopes of the lg $J/T^2 - T^{-1}$ plots for each mesomorphic phase were practically similar to those in figure 5 ($\varphi_{BN} = 0.37 \pm 0.05$ V, $\varphi_{BI} = 0.92 \pm 0.05$ V). For '+'Cu-Z+2-wt-%-D$_2$-RP'−', the temperature dependences of J/T^2 practically coincide with those obtained for In$_2$O$_3$-Z+2 wt % D$_2$-In$_2$O$_3$ ($\varphi_{BN} = 0.88 \pm 0.05$ V, $\varphi_{BI} = 0.70 \pm 0.05$ V). Thus, we can make a very important conclusion: the carrier transport across the LC–electrode interface is controlled by the barrier at the anode.

As mentioned above, such a barrier corresponds to electron transfer from the LC to the electrode. To analyse such a transport, it is important to find out which of the contacting bodies (LC or electrode) mainly determines φ_B. This can be done by analysing φ_B values for different electrodes and mesomorphic phases. If LC molecules are not aligned (isotropic phase), φ_{BI} values vary between different electrodes to a much lesser extent than φ_{BN} for the planar and homeotropic alignment of LC molecules. Hence follows one more very important conclusion: the barrier height is mainly determined by the properties of LC molecules.

If we assume that the barrier height obtained from temperature measurements is related to electron transfer from a cation to the electrode, a question immediately arises concerning the continuity of the charge exchange between the electrodes. A negative ion that has lost its electron at the anode becomes a neutral molecule and is no more involved in charge transport. The current flow through the sample must decrease the concentrationof the negative ions at the cathode and increase the number of neutral molecules at the anode. Therefore, the current arising at the instant of switching-on the voltage must fall practically to zero very rapidly, which contradicts the experimental data.

For the charge exchange between the electrodes to be continuous, we must assume that a negative ion reaching the anode donates not only an 'extra' electron (transforming into a neutral molecule), but also an its 'own' electron (transforming into an positive ion). It is to this process of conversion of neutral molecules into positive ions that the main 'part' of the barrier corresponds. A cycle of charge transport by the same molecules will be closed if, having captured two or more electrons on reaching the cathode, the positive ion again becomes a negative ion.

If it is assumed that the basic process in the charge transport across the electrode–LC interface is ionization of neutral LC molecules, we must make several remarks concerning the application of the Schottky theory, developed for solids, to dielectric liquids. In the case of the 'solid-state' Schottky effect, the transport of an electron from metal through a dielectric is considered, whereas in our case an electron moves from weak electrolyte through a dielectric layer to an electrode. In the case of the solid-state Schottky effect, the electron motion is hindered by the image force. In the case of ionization of a neutral molecule this role is played by the force of interaction between an electron and the formed positive ion. Such interactions being described by identical expressions, we obtain the same $J - V$ dependences (expression (7)).

For the solid-state Schottky effect, the charge transport mechanism is frequently specified by analysis of the Richardson constant. For thermionic emission, the constant is given by [15]

$$A^* = \frac{4\pi e m^* k^2}{\hbar^3} \tag{9}$$

where m^* is the effective electron mass, and $\hbar$ is Planck's constant. Commonly, the m^*/m_0 ratio is considered, where m_0 is the free electron mass. Analysis of the obtained data indicates that the average m^*/m_0 value is within $10^{-3}-10^{-6}$. It is rather difficult to explain so small values in terms of the diffusion transport theory [15].

The dielectric layer at the electrode–LC interface is a dielectric liquid, instead of a solid dielectric. The electron transport through it, occurring by the hopping conduction mechanism, differs from that in solids. In this case, the decrease in the number of already excited electrons may be due both to recombination and to trapping by neutral molecules of the dielectric layer.

For the solid-state Schottky effect, the barrier height is determined by the difference between the electron work functions of a dielectric and a metal. In the model discussed here, an electron is detached from a neutral molecule into a condensed medium–liquid. This process requires energy equal to the difference between the ionization energy of a separate molecule, I_G, and that of molecules in the liquid as a condensed medium, I_C. According to the Lyons model [16]

$$I_G - I_C = P \tag{10}$$

where P is the energy of polarization of the nearest molecules by the electron. If we regard an electron generated by ionization and temporarily localized, during tunnelling, on a certain molecule as a point charge, and the dipole molecules induced by this electron as point dipoles, and neglect the dipole–dipole interactions, then we have in such a zero approximation [17],

$$P = \sum_{k=1}^{n-1} \frac{e^2 \delta}{2 r_k^4} \tag{11}$$

where n is the concentration of molecules, δ is the polarizability of molecules, r_k is the distance between the molecule on which the electron is temporarily localized to a particular polarized molecule. It follows from expression (11) that P generally depends on δ. Liquid crystals being an anisotropic medium, δ depends on how the charge moves with respect to molecule axes; δ is manly determined by $\delta_\perp$ for a planar orientation, and by $\delta_\parallel$ for the homeotropic alignment. For the investigated LCs with large $\Delta\varepsilon$, the values of $\delta_\perp$ and $\delta_\parallel$, and the corresponding dielectric constants, are essentially different. This leads to the experimentally observed large difference between the φ_{BN} values for the homeotropic and planar molecule alignments.

The above analysis qualitatively explains the differences in φ_{BN} between different molecule alignments. A more detailed analysis of the transport processes is necessary for making quantitative estimations, including not only the ionization of molecules at the anode, but also injection at the cathode. This will be the subject of further studies. It should be added that the estimates of P obtained in [3] ($P_\perp = 0.7$ eV, $P_\parallel = 2.1$ eV) are close to $e\varphi_B$. This is evidence in favour of the proposed mechanism.

Thus, the main process governing the current transport across the electrode–LC interface, is the emission of electrons from the LC volume (behaving as a weak electrolyte) through the dielectric layer to the electrode. Therefore, it is important to understand what processes result in the formation of a dielectric layer on the electrode surface. In the case when there are nearly neutral dye molecules in the LC, the reasons for the dielectric layer formation are trivial. It is more difficult to determine why such a layer is formed on the electrode surface in pure LC. It is believed that, as in the case of electrolytes, the EDL in LCs is formed through ion adsorption [12, 18–21]. To make estimates, let us assume that the carrier mobility in the LC under consideration is about 10^{-10} m^2 V^{-1} s^{-1}, as in most other liquid crystals [10, 22]. Let us further assume that all the available ions from the sample volume of thickness $20\,\mu$m are adsorbed onto the electrode surface and the ion diameter is 1 nm. Then, a 1-nm-thick layer is formed on the electrode surface for a more conductive mixture Z+2 wt % D$_2$. Since

only a minor part of ions present in the bulk are adsorbed on the electrode surface, the actual thickness of this layer must be much less than 1 nm.

At $U < 1$ V almost the entire voltage is applied to the near-electrode region; therefore,

$$U = Ed_\mathrm{d} \tag{12}$$

where E is the electric field strength, and d_d is the thickness of the dielectric layer. Hence [12],

$$\beta = \frac{e}{kT} \left(\frac{e}{4\pi \varepsilon \varepsilon_0 d_\mathrm{d}} \right)^{1/2} \tag{13}$$

where ε_0 is the permittivity of vacuum, and ε is the dielectric constant of the substance. As follows from table 2, d_d values calculated using expression (13) exceed the estimates made in the roughest approximation. Moreover, the dielectric layer thickness for B is even greater than that for B+0.8 wt % D_1. Therefore, it is necessary to assume that even in pure LC there are neutral impurities with concentration much exceeding that of ions. Such impurities, being adsorbed together with ions, form a dielectric layer that hinders direct contact between ions and the electrode, defining the charge transport mechanism. As already mentioned, neutral impurities in pure LC may have varied origin (molecules of gases, photooxidation and synthesis products, etc.). Therefore, the electric strength of the dielectric layer formed through adsorption is poor. This accounts for the dramatic change in β and J_0 under the action of an external electric field. The introduction of dye molecules results in the formation of an adsorbed layer with more uniform composition, and the parameters becomes significantly more stable.

Let us further consider the relationship between various near-electrode relaxation processes, studied by the LFSD method, and the mechanism of charge transport across the LC–electrode interface. The data in tables 1 and 2 indicate that the W and d_d values are practically the same for all the materials studied. Therefore, the near-electrode relaxation processes are also due to carrier transport across the electrode–LC interface. The slower the charge transport, the more prolonged are processes of ion redistribution in the near-electrode region. Therefore, the dielectric relaxation time must be close to, or coincide with, the charge transport time. Since the charge transport is controlled by tunnelling, the dielectric relaxation time must follow the exponential dependence on reciprocal temperature. This conclusion is fully confirmed by earlier data [3]. For further substantiation of this conclusion, it is necessary to determine the activation energy of τ and compare it with $e\varphi_\mathrm{B}$. This will be the immediate subject of further studies.

5. Conclusions

- Both in pure LC and in solutions of dyes in LCs, almost the entire voltage is applied to the near-electrode region at $U < 1$ V. The voltage redistribution in the sample can be analysed using the polarization voltage concept. The dc conductance σ_dc was found in terms of this model. Close magnitudes of σ_dc and σ_ac confirm the applicability of the chosen model to analysis of the voltage redistribution.
- The carrier transport across the LC–electrode interface is described by the Schottky emission through a thin dielectric layer. The thickness of such a layer changes upon dye introduction and decreases under prolonged action of an external electric field. The reasons why the sample parameters change under the action of electric field were discussed and methods for stabilizing these parameters were proposed.
- A thin dielectric layer is formed through adsorption of both ions and neutral impurity molecules onto the electrode surface. According to the estimations made, the concentration of such molecules is much higher than that of ions even in pure LC.

- The basic mechanism of carrier transport through the barrier involves transfer of an electron from an LC molecule to the electrode. Specific features of such a transport in dielectric liquids were discussed in comparison with the Schottky emission in solids. An assumption was made that the continuity of charge exchange in the LC bulk, involving the same ions, is due to changes in their polarities (cation–anion or *vice versa*) at each electrode.
- The high ε' and ε'' values in the low-frequency dispersion domain are due to voltage redistribution. The lower the frequency, the narrower the region of the near-electrode layer to which the voltage is applied.
- The low-frequency relaxation processes are caused by carrier transport across the LC–electrode interface. This is confirmed by the practically coinciding thickness W of the diffusion region in the EDL and the thickness d_d of the dielectric layer, and by the Arrhenius behaviour of the tunnel current J and the dielectric relaxation time τ.

Acknowledgments

References

[1] Sprokel G J 1973 *Mol. Cryst. Liq. Cryst.* **22** 249
[2] Koval'chuk A V 1996 *Ukr. Fiz. Zh.* **41** 991
[3] Koval'chuk A V 1996 *Ukr. Fiz. Zh.* **41** 1093
[4] Hitoshi Mada and Masahiro Ryuzaki 1995 *Japan. J. Appl. Phys.* **34** L1134
[5] Shuichi Murakami, Hironori Iga and Hiroyoshi Naito 1996 *J. Appl. Phys.* **80** 6396
[6] Koval'chuk A V 1998 *J. Chem. Phys.* **109** 8190
[7] Koval'chuk A V 1998 *Functional Materials* **5** 426
[8] Koval'chuk A V 1999 *Ukr. Fiz. Zh.* **44** 1376
[9] Koval'chuk A V 2000 *JETP Lett.* **72** 377
[10] Blinov L M 1983 *Electro-optical and Magneto-optical Properties of Liquid Crystals* (New York: John Wiley)
[11] Baizer M M (ed) 1973 *Organic Electrochemistry* (New York: Marcel Dekker)
[12] Hitoshi Mada and Shigero Yoshino 1988 *Japan. J. Appl. Phys.* **27** L1361
[13] Yudin S G, Blinov L M and Petukhova N N 1999 *JETP Lett.* **70** 633
[14] Koval'chuk A V 2000 *Tech. Phys. Lett.* **26** 559
[15] Sze S M 1981 *Physic of Semiconductor Devices* (New York: Wiley Interscience)
[16] Gutman F and Lyons L E 1967 *Organic Semiconductor* (New York: Wiley Interscience)
[17] Silinsh E A 1980 *Organic Molecular Crystals. Their Electronic States* (Berlin: Springer)
[18] Barbero G and Durand G 1990 *J. Appl. Phys.* **67** 2678
[19] Barbero G and Durand G 1999 *J. Phys. France* **51** 281
[20] Barbero G, Zvezdin A K and Evangelista L R 1999 *Phys. Rev.* E **59** 1846
[21] Nazarenko V G, Pergamenshchik V M and Koval'chuk O V 1999 *Phys. Rev.* E **60** 5580
[22] Grisenko N I and Moshel N V 1980 *Ukr. Fiz. Zh.* **25** 1830